Influence of Atomizer Exit Area Ratio on the Breakup Morphology of Coaxial Air and Round Water Jets

Hui Zhao, Hai-Feng Liu, Xiu-Shan Tian, Jian-Liang Xu, and Wei-Feng Li
Key Laboratory of Coal Gasification and Energy Chemical Engineering of Ministry of Education, Dept. of Chemical Engineering for Energy and Resources, East China University of Science and Technology, Shanghai 200237, P.R. China

Shanghai Engineering Research Center of Coal Gasification, Dept. of Chemical Engineering for Energy and Resources, East China University of Science and Technology, Shanghai 200237, P.R. China

Kuang-Fei Lin
State Environmental Protection Key Laboratory of Environmental Risk Assessment and Control on Chemical Process, Dept. of Environmental Engineering, East China University of Science and Technology, Shanghai 200237, P.R. China

DOI 10.1002/aic.14414
Published online February 25, 2014 in Wiley Online Library (wileyonlinelibrary.com)

The goal of this article is to study the effect of atomizer exit area ratio on atomizer performance. The experiments are performed on the round liquid jet breakup of seven coaxial air-blast atomizers with water–air systems. The breakup morphology of liquid jet is observed first. The membrane-type breakup can be divided into two subregimes called bag-type breakup and membrane-fiber breakup, and a correlation of characteristic length on bag-type breakup regime is obtained. Then, we analyze the influence of atomizer exit area ratio on the breakup morphology of water-air jets. To obtain reasonable atomization morphology criterions, the atomizer exit area ratio is used to modify the Weber number and momentum flux ratio per unit volume. This method is found to be able to explain different experimental results in the literature, which is also close to the results of round liquid jet in cross air flow and secondary atomization. © 2014 American Institute of Chemical Engineers *AIChE J*, 60: 2335–2345, 2014
Keywords: air-blast, coaxial, sprays, atomization, breakup

Introduction

The transformation of liquid into spray is of importance in many industrial chemical processes. The liquid jet breakup and atomization is a complicated multiparameter two-phase flow problem which resists clear understanding. Many investigations have been made since Rayleigh.[1] Atomization has been extensively studied both theoretically and experimentally, including Hinze,[2] Reitz and Bracco,[3] Lefebvre,[4] Villermaux,[5] and Liu et al.[6] and so forth. Due to numerous applications, atomization has received significant attention. Several review papers have been done by Lasheras and Hopfinger,[7] Villermaux,[8] Gorokhovski and Herrmann,[9] and Dumouchel.[10] The liquid atomization is also a fundamental research topic in multiphase flow.[11–15]

In the studies of coaxial air–water jets, liquid Reynolds number *Re*, gas Weber number *We*, and momentum flux ratio per unit volume *M* have been considered as main parameters. The liquid Reynolds number is a dimensionless number that gives a measure of the ratio of inertial forces to viscous forces

$$Re=\frac{\rho_l D u_l}{\mu_l} \tag{1}$$

where u_l, μ_l, and ρ_l are the velocity, dynamic viscosity, and density of liquid, respectively, D is the exit diameter of liquid jet. The gas Weber number represents the ratio of disruptive aerodynamic force to the stabilizing surface tension force

$$We=\frac{\rho_g D(u_g-u_l)^2}{\sigma} \tag{2}$$

where ρ_g and u_g is the density and velocity of gas, respectively, σ is surface tension. The momentum flux ratio per unit volume is given by

$$M=\frac{\rho_g u_g^2}{\rho_l u_l^2} \tag{3}$$

Gas to liquid mass ratio (GLR) is also an important parameter on the air-blast atomization. The expression of GLR is $\mathrm{GLR}=\frac{\rho_g u_g A_g}{\rho_l u_l A_l}$, where A_g/A_l is the area ratio of gas exit and water exit.

Farago and Chigier[16] propose a morphological classification of disintegrating coaxial air–water jets. Four main atomization regimes are identified: the Rayleigh-type breakup ($We<25$), the membrane-type breakup ($25<We<70$), the

Correspondence concerning this article should be addressed to H.-F. Liu at hfliu@ecust.edu.cn.

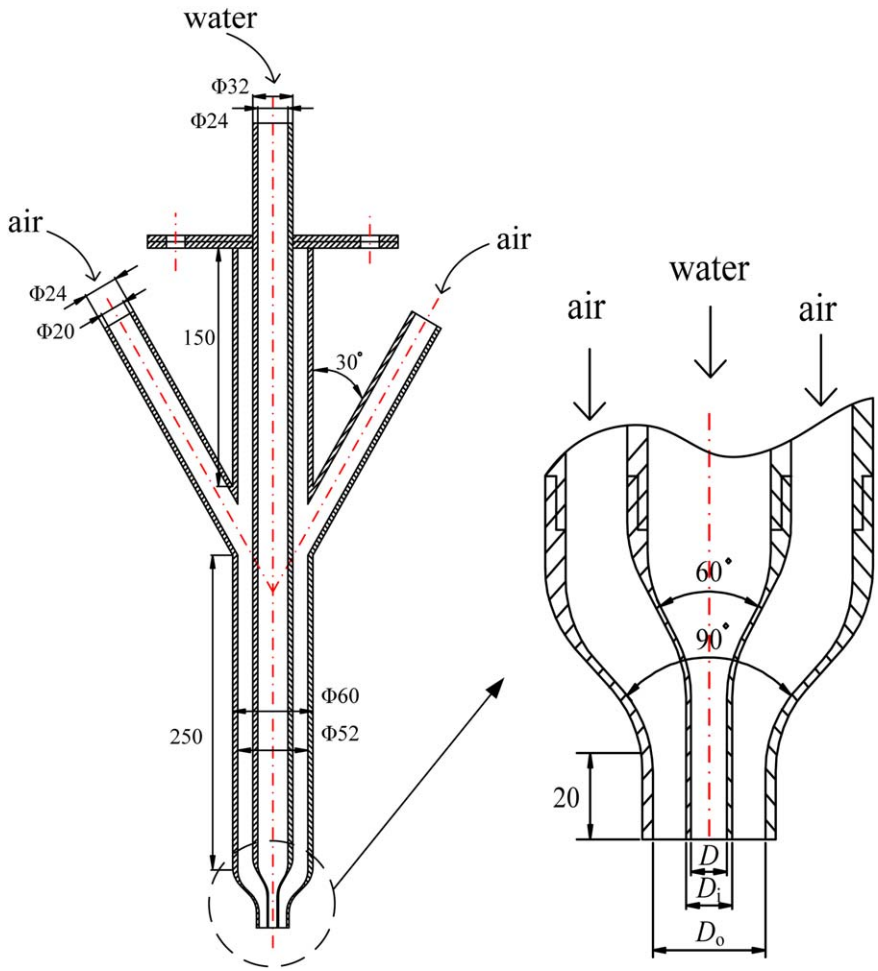

Figure 1. Coaxial two-fluid air-blast atomizer configuration.

(dimensions are in mm). [Color figure can be viewed in the online issue, which is available at wileyonlinelibrary.com.]

fiber-type breakup ($We > 70$), and the superpulsating breakup ($Re/\sqrt{We} < 100$). The Rayleigh-type breakup can be divided into two subregimes called axisymmetric ($We < 15$) and non-axisymmetric ($15 < We < 25$). They succeed in classifying these breakup regimes in a *We–Re* map with their atomizer. Lasheras and Hopfinger[7] summarize the results in the literature and obtain a breakup regime in the parameter space *We–Re*. Lasheras et al.[17] also study the atomization characteristics of liquid jet primary breakup. However, because of difference in the atomizer geometry, the range of breakup regime in Lasheras et al.[17] do not agree well with the results of Farago and Chigier.[16]

In the atomization of coaxial air and round water jet, the important influential factors are: gas velocity u_g, water velocity u_l, water exit diameter D, gas exit diameter D_o, and fluid physical properties. Based on the definitions of dimensionless numbers in *We* and *Re,* the parameter of gas exit diameter D_o is neglected. The influence of water–air exit area ratio of atomizer is not considered. So the *We–Re* map needs to be improved. Subsequently, Leroux et al.[18] investigate the behavior of coaxial liquid jets produced by nine different atomizers. They suggest categorizing the primary breakup mechanism in a M–Re_g map, where M is the momentum flux ratio $M=\rho_g u_g^2/(\rho_l u_l^2)$ and Re_g is the gas Reynolds number $Re_g=\rho_g D_o u_g/\mu_g$, where μ_g is the dynamic viscosity of gas. This suggestion is found appropriate to dissociate the Rayleigh-type breakup regime and the superpulsating breakup regime but could not dissociate the membrane-type breakup regime and fiber-type breakup regime. This is due to neglecting the water exit diameter, D, in the M–Re_g map.

Recently, the experimental results on membrane-type breakup regime of Wang et al.[19] and Baillot et al.[20] (Baillot et al.[20] have done the experiments both without acoustics and with acoustics, respectively. The data of Baillot et al.[20] cited in this article are the experimental results without acoustics.) do not agree with the experimental results of Farago and Chigier.[16] The different results are also due to their different atomizer exit diameters. So owing to the complexity of the underlying physical processes involved in the breakup of liquid–gas jets, some influencing factors, especially the effect of atomizer exit diameter on transition *We* are still poorly understood.

The self-similar behaviors of atomization at different length scales open a new perspective on this classical problem in recent years.[21,22] Wang et al.[19] notice that the similarity between the primary and secondary air-assisted liquid jet breakup mechanisms when they study the transition of liquid jet from a ligament-mediated to a membrane-mediated breakup. This indicates the self-similar behavior is a universal rule of atomization. This experiment also shows the membrane-type breakup of coaxial water–air jets plays an important role in the atomization self-similar behavior. And

Table 1. Dimensions of Atomizers

Atomizer No.	D (mm)	D_i (mm)	D_o (mm)	A_l/A_g
1	9.02	11.14	14.92	0.826
2	5.10	7.12	9.32	0.719
3	4.02	6.28	14.92	0.088
4	2.00	4.24	14.92	0.020
5	2.00	3.90	23.88	0.007
6	4.02	6.08	23.88	0.030
7	6.96	9.04	23.88	0.099

the detailed properties of membrane-type breakup have not been completely known until now.

In this article, the breakup morphology of water–air jets is observed first using high-speed camera. And the characteristics of bag-type breakup have been investigated. Then, the modified *We–M* map on coaxial water–air jets breakup regimes is obtained. The similar behavior in different processes of atomization is studied at last.

Experimental Apparatus and Methodology

The coaxial two-fluid air-blast atomizer geometry is shown schematically in Figure 1, consisting of the geometrically simple case of a round liquid jet surrounded by a coflowing annular air stream. It is similar to our earlier work.[23,24] There is no flow straightener in the upstream of the atomizer. There are seven kinds of atomizers used in this experiment, and their dimensions are indicated in Table 1. The results of atomizer diameter reported in Table 1 are measured by Vernier caliper, whose uncertainty is ±0.02 mm. The minimum dimension in Table 1 is 2.00 mm, so the uncertainty is within ±1%. Liquid phase passes through the central passage while the gas phase passes through the annular space. A_l/A_g is the area ratio of water exit and gas exit. The experiments are conducted at atmospheric pressure and room temperature, and the working fluids are water and air.

The experimental apparatus is sketched in Figure 2. The type of flow meters used is LZB glass tube rotameter flow meter, whose uncertainty is ±1.5%. We begin testing after

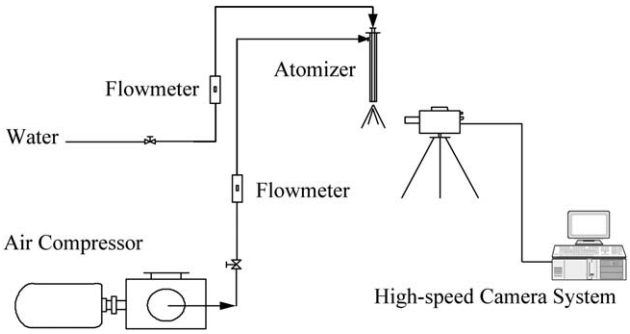

Figure 2. Sketch of the experimental apparatus.

the float (weight) in tube of flow meter is steady. The type of high-speed camera is Fastcam APX-RS from Photron. In this test, the image resolution is 1024 × 512 pixels, and the framing rate is 1000 images per second. The type of halogen lamp is QH-H1300 from Wenzhou Changcheng Photo-Facility Co.

In the experiment, M is in the range of 0.011–620, We is in the range of 8.8–455, Re is in the range of 783–35,100, and GLR is in the range of 0.012–12. Based on the method of Klein and McClintock,[25] the uncertainty of A_l/A_g is ±2%, the uncertainty of GLR is ±5%, the uncertainty of M is ±7%, the uncertainty of We is ±6%, and the uncertainty of Re is ±3%.

Results and Discussion

Morphology classification

Based on the definition in the literature,[16] the membrane-type breakup is characterized by the formation of a thin sheet, and the fiber-type breakup is characterized by the formation of liquid fibers. However, there is the transition condition which has fiber structure and sheet structure at the same time. To make the classification of breakup mechanism more reasonable, here we suggest the transition condition can be named the membrane-fiber breakup. When thin sheet

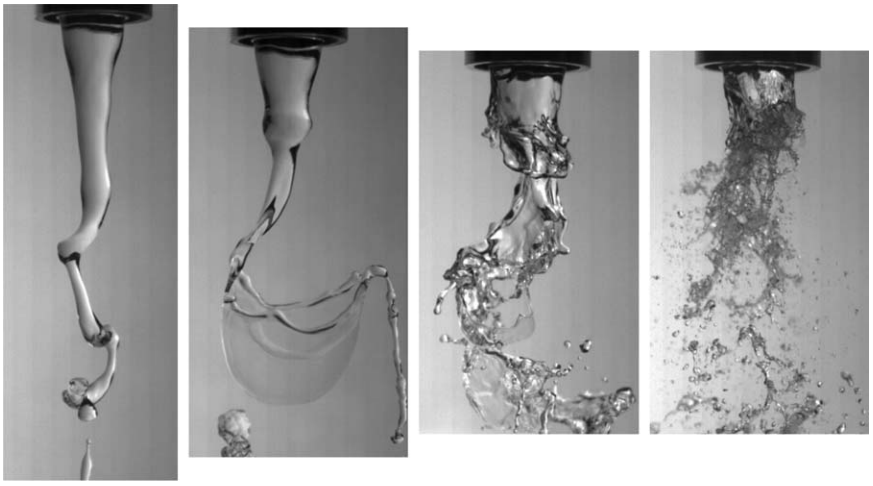

Figure 3. Sketch of different breakup mechanisms.

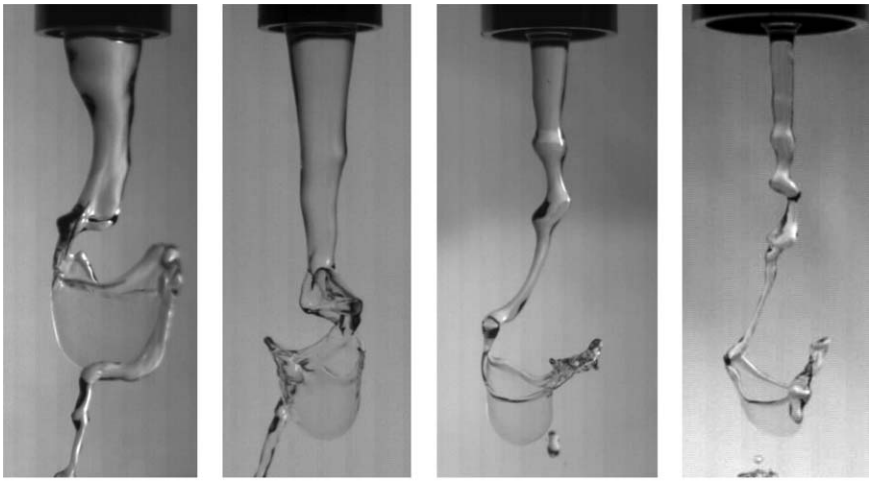

(a) Atomizer 1, u_l=0.17m/s, u_g=18.0m/s; (b) Atomizer 2, u_l =0.41m/s, u_g =24.4m/s; (c) Atomizer 3, u_l=0.44m/s, u_g =15.4m/s; (d) Atomizer 4, u_l=0.88m/s, u_g =21.6m/s

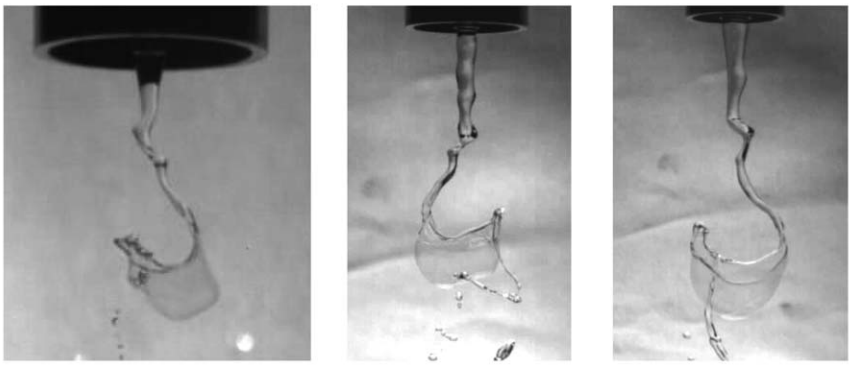

(e) Atomizer 5, u_l=0.53m/s, u_g=22.3m/s; (f) Atomizer 6, u_l =0.88m/s, u_g =16.6m/s; (g) Atomizer 7, u_l=0.29m/s, u_g =14.5m/s

Figure 4. Photographs of bag-type breakup.

is the only characteristic structure, we suggest this breakup can be named as the bag-type breakup. Similar to the bag breakup of secondary atomization, the thin hollow bag structure is the main characteristic of bag-type breakup. The membrane-fiber breakup can be considered as the transition breakup regime between bag-type breakup and fiber-type breakup.

The breakup morphology of coaxial air and round water jets is shown in Figure 3. The experimental photographs of bag-type breakup and membrane-fiber breakup are shown in Figures 4 and 5, respectively. We divide the membrane-type breakup in two subregimes, which is also convenient to compare the breakup regimes of coaxial air–liquid jet, liquid jet in air crossflow, and secondary atomization. This content will be shown in section comparison of breakup regimes in different conditions.

In bag-type breakup, the air flow is strong enough to make the liquid jet oscillate. When the air flow and the oscillating part of liquid jet are vertical, the air flow impacts on the oscillating part of the liquid jet directly, where the air pressure makes the oscillating part of liquid jet deform from cylinder to sheet-like shape. Then the center of the sheet deforms into a thin membrane-like bag and the bag progressively breaks up from its bag toward the basal ring. Figure 6 shows the experimental photographs of bag-type breakup whose time interval is 2 ms.

In bag-type breakup, during the bag development and breakup period, the position of bag keeps changing. Here, we define that the characteristic length L in bag-type breakup is the distance between atomizer exit and the position where bag structure appears first as shown in Figure 6. This characteristic length L can be also considered as the minimum distance between atomizer exit and the bag position during the bag development and breakup period. The best fit correlation of the present measurements (all bag-type breakup data of seven atomizers) is given by

$$\frac{L}{D}=5.2\left(\frac{A_{\mathrm{l}}}{A_{\mathrm{g}}}\right)^{-0.17}M^{-0.28} \tag{4}$$

The correlation coefficient of the fit is 0.93. Equation 4 shows that the dimensionless characteristic length L/D decreases with the parameters $A_{\mathrm{l}}/A_{\mathrm{g}}$ and M, and the effect of M is bigger than $A_{\mathrm{l}}/A_{\mathrm{g}}$. L/D values calculated using this correlation are plotted against the measured values in Figure

(a) Atomizer 1, u_l=0.17m/s, u_g=26.9m/s

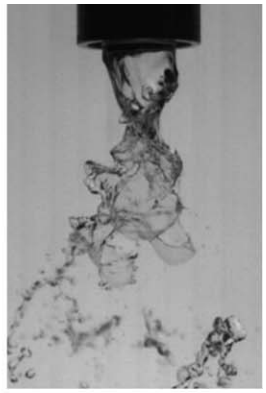

(b) Atomizer 2, u_l =0.41m/s, u_g =39.1m/s

(c) Atomizer 3, u_l=0.88m/s, u_g =23.2m/s

(d) Atomizer 4, u_l=1.95m/s, u_g =34.6m/s

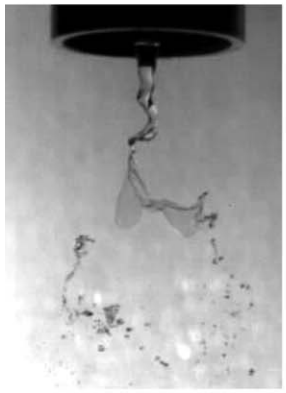

(e) Atomizer 5, u_l=0.88m/s, u_g=28.7m/s

(f) Atomizer 6, u_l =0.88m/s, u_g =23.2m/s

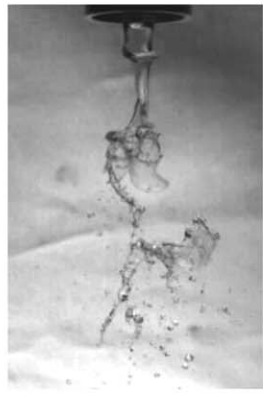

(g) Atomizer 7, u_l=0.44m/s, u_g =21.7m/s

Figure 5. Photographs of membrane-fiber breakup.

7. The correlation of Leroux et al.[18] on the characteristic length L is

$$\frac{L}{D}=10M^{-0.3} \tag{5}$$

In the experiment of Leroux et al.,[18] the range of $\left(\frac{A_l}{A_g}\right)^{-0.17}$ is 1.0–2.8, so the average of $\left(\frac{A_l}{A_g}\right)^{-0.17}$ is about 1.9. Then, based on Eq. 4 there is

$$\frac{L}{D}=5.2\left(\frac{A_l}{A_g}\right)^{-0.17}M^{-0.28}\approx 5.2\times 1.9M^{-0.28}\approx 9.9M^{-0.28} \tag{6}$$

So the previous work is close to our results.

S-type means that the shape of liquid cylinder is like the letter "S." The cylindrical liquid jet may be sinuous and show S-type, so two parts of liquid jet would be vertical to the airflow. Sometimes there are two bags appearing at the same time as shown in Figure 8.

Breakup regime range

The aerodynamic Weber number We is one of the most important parameters in the classification of atomization modes, and M, GLR, and A_l/A_g are also important parameters. Breakup regimes observed in this test are shown in Figure 9 (high M) and Figure 10 (low M), respectively. In Figures 9a and 10a, the horizontal ordinate is GLR, so the

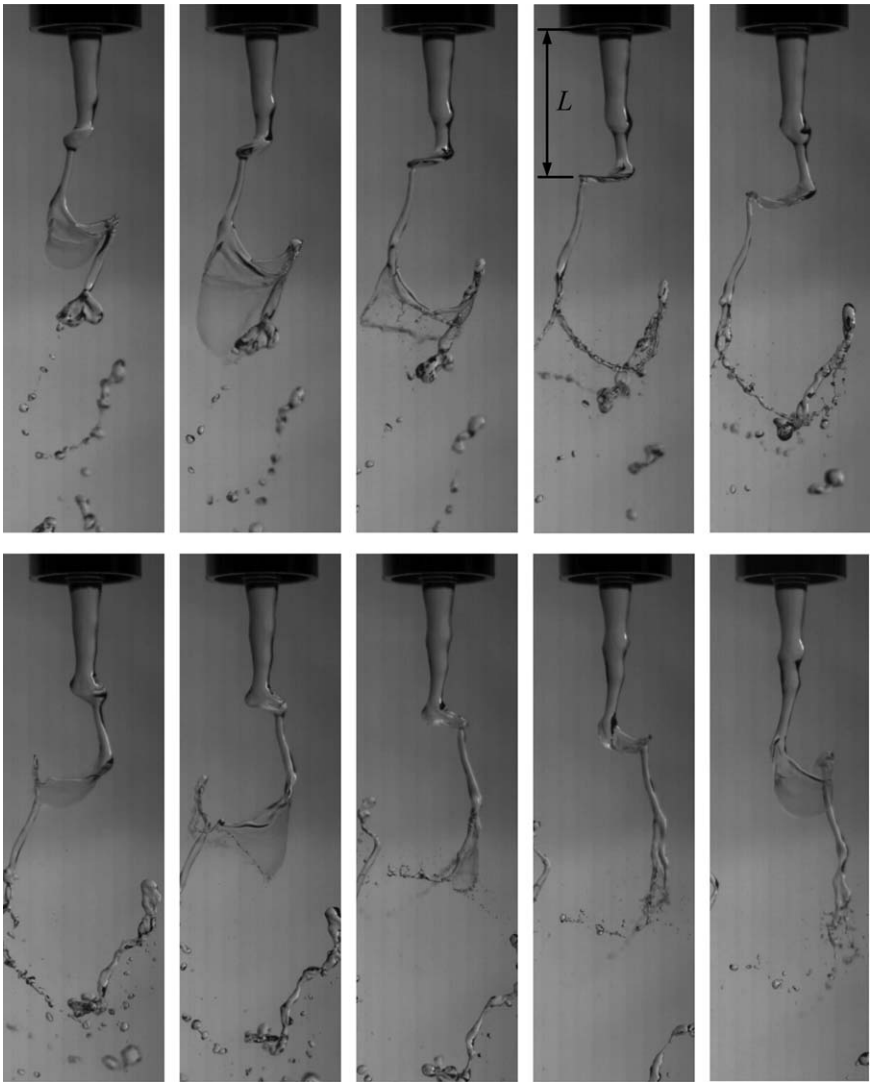

Figure 6. A serial experimental photograph of bag-type breakup, the time interval is 2 ms.

influence of GLR can be observed directly. The experimental results show that at high GLR the transition *We* changes little with GLR, and at low GLR the transition *We* decreases with GLR. To obtain the same breakup morphology, the atomizer with smaller GLR would need larger transition *We*.

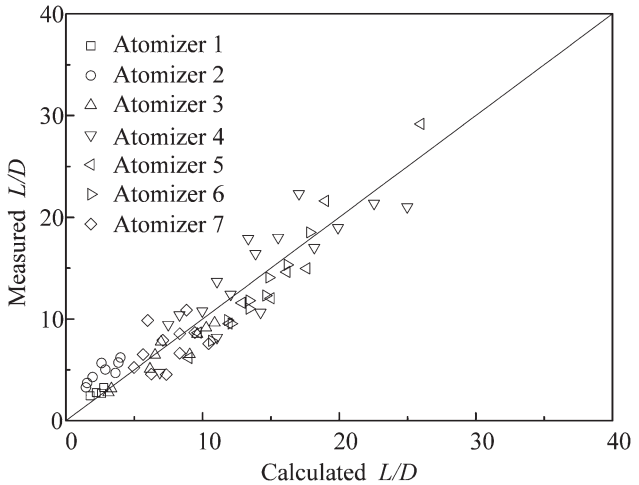

Figure 7. Comparison of measured *L/D* to *L/D* predicted by Eq. 4.

Energy approach is often used in the analysis of atomization.[26] Here, the energy needed by water jet breakup comes from the kinetic energy of airflow basically. The total input energy supplied by airflow is E_t. The large part of the input energy, E_0, with two-fluid atomizer is used to accelerate the liquid; and small part of the input energy, E_1, is used to make the liquid deformation and breakup. Here, we suggest the input energy is distributed proportionately. So there is

$$E_t = E_0 + E_1 \tag{7}$$

and

$$E_0/E_1 \approx \text{constant} \tag{8}$$

Then, we assume that E_2 is the energy supplied by airflow when GLR $\rightarrow \infty$ or $A_l/A_g \rightarrow 0$. So when the GLR is big enough or A_l/A_g is small enough, there is

$$E_1 \approx E_2 \tag{9}$$

However, a lot of atomizers hold a small value of GLR or a big value of A_l/A_g, the effect of boundary layer is great.

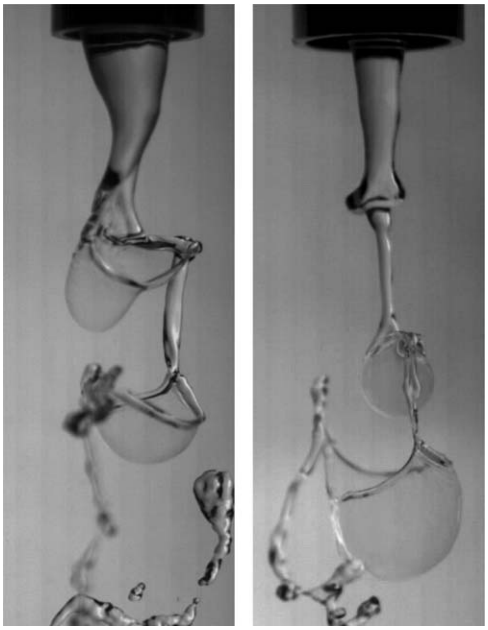

Figure 8. Dual bags in bag-type breakup.

The surrounding still air would dissipate the energy E_3 of airflow and make the inner air velocity decrease. So there is

$$E_1 \approx E_2 + E_3 \tag{10}$$

The energy comes from the aerodynamic force, so there is

$$E_1 \propto We_t \tag{11}$$

and

$$E_2 \propto We_0 \tag{12}$$

where We_t is the transition We between different breakup modes, and We_0 is the transition We when GLR $\rightarrow \infty$ or $A_l/A_g \rightarrow 0$. We assume that the energy E_3 of airflow dissipated by the surrounding still air would decrease with the increase GLR, so there is approximately

$$E_3 \propto kWe_0/\mathrm{GLR} \tag{13}$$

Then, we can obtain that

$$We_t = We_0(1 + k/\mathrm{GLR}) \tag{14}$$

where k is a correction factor. GLR is widely used in the prediction of mean diameter (for instance Sauter mean diameter, SMD) in air-blast atomization. The relationship between dimensionless SMD and We can be expressed as generally[4]

$$\frac{\mathrm{SMD}}{D} \propto We_0^{-x} \tag{15}$$

where x is a correction factor. Based on the suggestion of Eq. 14, there is approximately

$$\frac{\mathrm{SMD}}{D} \propto \left(\frac{We_t}{1 + k/\mathrm{GLR}}\right)^{-x} \propto We_t^{-x}(1 + k/\mathrm{GLR})^x \tag{16}$$

When the viscosity of test liquid could be neglected, the correlation of experimental results in the literature[27] is

$$\frac{\mathrm{SMD}}{D} = 0.48We^{-0.4}\left(1 + \frac{1}{\mathrm{GLR}}\right)^{0.4} \tag{17}$$

Equations 16 and 17 are very similar, this indicates that our suggestion agrees with the data in the literature and the suggestion is reasonable.

Based on Eq. 14, the best fit correlations of the experimental results on the transition of breakup types at $M > 0.08$ are

$$We_1 = 15\left(1 + \frac{0.03}{\mathrm{GRL}}\right) \tag{18}$$

$$We_2 = 28\left(1 + \frac{0.03}{\mathrm{GRL}}\right) \tag{19}$$

$$We_3 = 90\left(1 + \frac{0.03}{\mathrm{GRL}}\right) \tag{20}$$

where We_1 is the transition Weber number between Rayleigh breakup and bag breakup; We_2 is the transition Weber number between bag breakup and membrane-fiber regime; We_3 is the transition Weber number between membrane-fiber regime and fiber breakup. The best fit correlations of the experimental results on the transition of breakup types at $M < 0.08$ are

$$We_4 = 28\left(1 + \frac{0.2}{\mathrm{GRL}}\right) \tag{21}$$

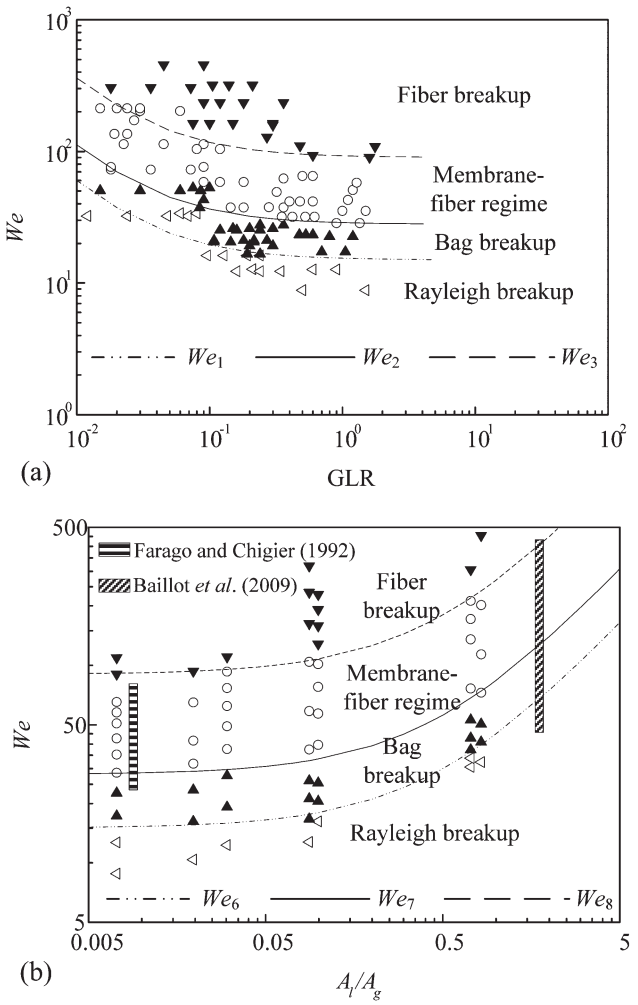

Figure 9. Breakup regimes in the parameter space (a) *We*-GLR (b) *We*-A_l/A_g at $M > 0.08$.

The shadow is the bag breakup and membrane-fiber regime range in the literature.

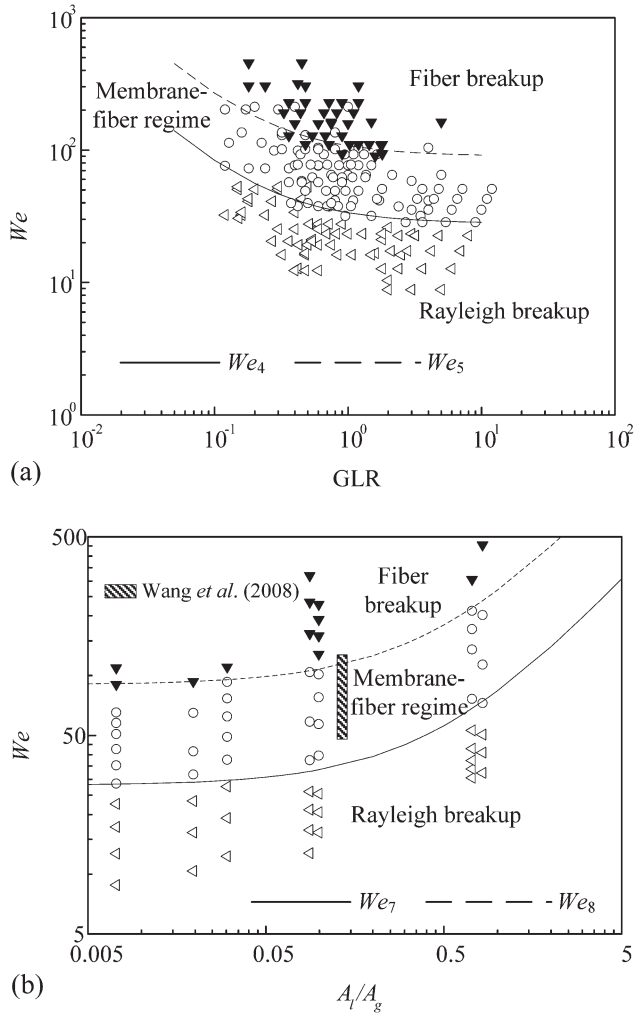

Figure 10. Breakup regimes in the parameter space (a) *We*-GLR (b) *We*-A_l/A_g at $M < 0.08$.

The shadow is the membrane-fiber regime range in the literature.

$$We_5 = 90\left(1 + \frac{0.2}{\mathrm{GRL}}\right) \tag{22}$$

where We_4 is the transition Weber number between Rayleigh breakup and membrane-fiber regime; We_5 is the transition Weber number between membrane-fiber regime and fiber breakup. The corresponding results are shown in Figures 9a and 10a, respectively.

In Figures 9b and 10b, the horizontal ordinate is A_l/A_g, so the influence of atomizer exit area ratio can be observed directly. The experimental results show that at low A_l/A_g the transition *We* changes little with A_l/A_g, and at high A_l/A_g the transition *We* increases with A_l/A_g. To obtain the same breakup morphology, the atomizer with larger A_l/A_g would need larger transition *We*.

Then, we analyze the influence of atomizer exit area ratio A_l/A_g on the air-blast atomization. We assume that the energy E_3 of airflow dissipated by the surrounding still air would increase with the increase A_l/A_g, so there is approximately

$$E_3 \propto K\frac{A_l}{A_g}We_0 \tag{23}$$

where K is a correction factor. So we can obtain that

$$We_t = We_0\left(1 + K\frac{A_l}{A_g}\right) \tag{24}$$

And the best fit correlations of the experimental results are

$$We_6 = 15\left(1 + 1.4\frac{A_l}{A_g}\right) \tag{25}$$

$$We_7 = 28\left(1 + 1.4\frac{A_l}{A_g}\right) \tag{26}$$

$$We_8 = 90\left(1 + 1.4\frac{A_l}{A_g}\right) \tag{27}$$

where We_6 is the transition Weber number between Rayleigh breakup and bag breakup; We_7 is the transition Weber number between bag breakup and membrane-fiber regime at $M > 0.08$, and the transition Weber number between Rayleigh breakup and membrane-fiber regime at $M < 0.08$; We_8 is the transition Weber number between membrane-fiber regime and fiber breakup. We obtain the linear coefficient K in Eq. 24, and in Eqs. 25–27 K is 1.4 by the experimental data fitting.

Farago and Chigier[16] define that the superpulsating mode as being characterized by the extremely high periodical change between low and high-density regions in the sprays. The effect of M on bag-type breakup and superpulsating breakup is huge. In the condition of GLR $\to \infty$ or $A_l/A_g \to 0$, when M is very big ($M > 20$),[16,18] it is the superpulsating breakup. When M is medial ($0.08 < M < 20$), there are four atomization regimes, which are Rayleigh-type breakup, bag-type breakup, membrane-fiber breakup, and fiber-type breakup. However, when M is small ($M < 0.08$), bag-type breakup will disappear. This is due to the airflow having difficulties making the liquid jet oscillate when the inertia of liquid jet is huge. So the breakup regimes will be Rayleigh-type breakup, membrane-fiber breakup, and fiber-type breakup at small M.

As shown in Figure 11a, the critical M of bag-type breakup appearing in view of GLR is

$$M_c = 0.08\left(1 + \frac{0.2}{\mathrm{GLR}^3}\right) \tag{28}$$

M_c decreases with the increase of GLR rapidly. We also find that the critical M of bag-type breakup appearing increases with A_l/A_g. As shown in Figure 11b, the critical M of bag-type breakup appearing in view of A_l/A_g is

$$M_c = 0.08\left(1 + 50\frac{A_l}{A_g}\right) \tag{29}$$

In the suitable range of *We*, if M is bigger than the critical M, there would be bag-type breakup. Otherwise bag-type breakup would not appear. Equation 29 is also consistent with the experimental results in the literature. The largest M of Wang et al.[19] is smaller than M_c, so the bag-type breakup will disappear in the test of Wang et al.[19] The range of M in Farago and Chigier[16] and Baillot et al.[20] is wide enough, so all breakup regimes will appear.

The ranges of breakup regimes in the literature[16,19,20] are also shown in Figures 9b and 10b. In Figure 9b, the breakup regimes in the parameter space *We*-A_l/A_g is at $M > 0.08$. The shadow is the bag-type breakup and membrane-fiber breakup regime range based on the data in the literature.[16,20] In

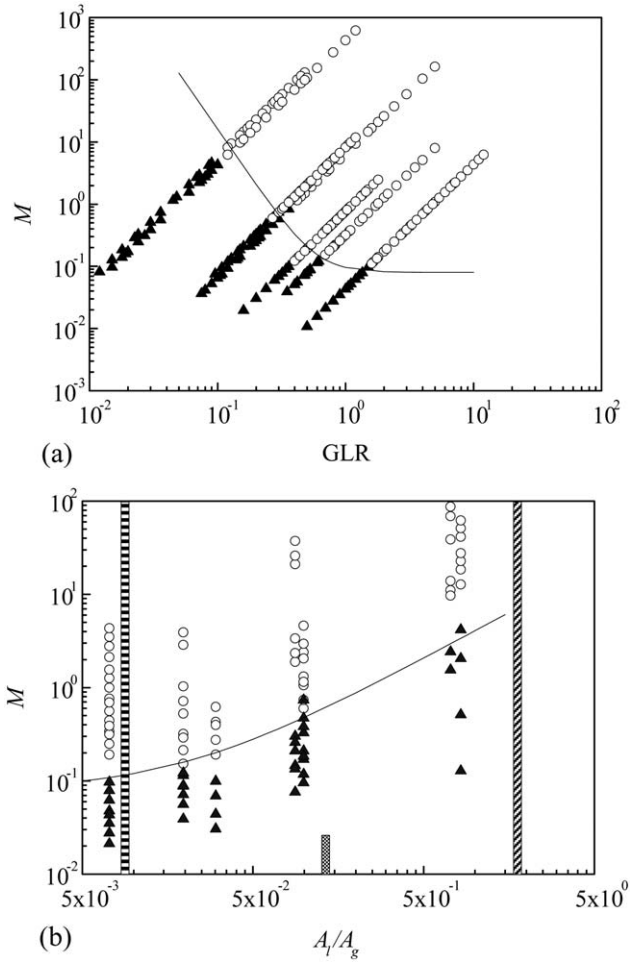

Figure 11. (a) The critical *M* of bag-type breakup appearing at different GLR.

○ bag-type breakup, ▲ no bag-type breakup. (b) The critical *M* of bag-type breakup appearing at different A_l/A_g. ○ bag-type breakup, ▲ no bag-type breakup. *M* range of Farago and Chigier,[16] *M* range of Wang et al.,[19] *M* range of Baillot et al.[20] The *M* range of Farago and Chigier[16] and Baillot et al.[20] is wide, so their results show bag-type breakup. The *M* range of Wang et al.[19] is smaller than the critical value, so their results do not show bag-type breakup.

Figure 10b, the breakup regimes in the parameter space We-A_l/A_g is at $M < 0.08$. The shadow is the membrane-fiber breakup regime range based on the data in the literature.[19] Note that the results of Farago and Chigier[16] and Baillot et al.[20] contain both bag-type breakup and membrane-fiber breakup. From Figures 9b and 10b, we can also find Eqs. 25–27 are in good agreements with those reported in the literature.[16,19,20] These correlations indicate that the influence of A_l/A_g is notable and can help us to explain the different values of transition We in the literature.

To consider the influence of A_l/A_g, we suggest using the modified We_m and M_m, which are

$$We_m = \frac{We}{1+1.4\frac{A_l}{A_g}} \tag{30}$$

and

$$M_m = \frac{M}{1+50\frac{A_l}{A_g}} \tag{31}$$

Equation 30 is obtained by Eqs. 25–27, and Eq. 31 is obtained by Eq. 29. The modified map is shown in Figure 12, in which the vertical lines are from Eqs. 25–27, so there are three vertical lines. And the horizontal line is from Eq. 29, so there is one horizontal line in Figure 12. The line in Figure 11b is the horizontal line in Figure 12. The same line shows different shapes in two figures are due to different vertical ordinates. In Figure 12, the broken line is the range of Wang et al.,[19] whose experimental results do not show bag-type breakup. The broken line is outside the region of bag-type breakup, so this also suggests that the We_m–M_m map is reasonable.

In We–Re map,[7,16,20] the parameter of air exit diameter D_o is neglected. In M–Re_g map,[18] the parameter of water exit diameter D is neglected. So these criterions in the literature can not reflect the impact of nozzle size and should be modified. To obtain reasonable atomization morphology criterions, we suggest using the atomizer exit area ratio to modify Weber number and momentum flux ratio per unit volume. In the new map of the parameter space We_m–M_m, all important parameters on nozzle size are considered.

Comparison of breakup regimes in different conditions

The research of similar behavior at different atomization conditions is interesting and important, which can help us to understand the mechanism of liquid breakup. Table 2 shows the comparison among the breakup regimes of air–water coaxial jets, liquid jet in cross air flow, and secondary atomization. The range of breakup regimes at different atomization conditions is close to each other.

The membrane-fiber breakup is characterized by the formation of fiber and sheet at the same time. As shown in Figure 13 (the experimental photograph of Sallam et al.[30]), it is a photograph of high-speed round liquid jet in still gas. The

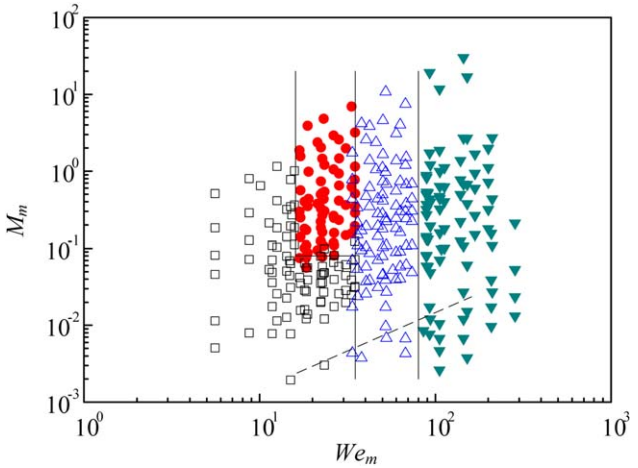

Figure 12. Breakup regimes in the parameter space We_m–M_m.

□ Rayleigh-type breakup, ● bag-type breakup, △ membrane-fiber breakup, ▼ fiber-type breakup. Solid line is the transition value of breakup types. And broken line is the range of Wang et al.,[19] whose results do not show bag-type breakup. [Color figure can be viewed in the online issue, which is available at wileyonlinelibrary.com.]

Table 2. Comparison of Breakup Regimes in Different Conditions

	Rayleigh-Type Breakup or Column Breakup	Bag-Type Breakup	Membrane-Fiber Breakup or Multimode Breakup	Fiber-Type Breakup or Shear Breakup
Air–liquid coaxial jet (at $A_l/A_g \to 0$)	$We < 15$	$15 < We < 28$	$28 < We < 90$	$We > 90$
Liquid jet in cross air flow[28]	$We < 4$	$4 < We < 30$	$30 < We < 110$	$We > 110$
Secondary atomization[29]	$We < 11$	$11 < We < 35$	$35 < We < 80$	$We > 80$

liquid jet has fiber structure and sheet structure at the same time, so it can be considered as membrane-fiber breakup. The condition of Figure 13 is

$$We_l = \frac{\rho_l D u_l^2}{\sigma} = 33100 \tag{32}$$

Here, we can change We_l into We. By assuming that $u_g = 0$, there is

$$We = \frac{\rho_g D (u_g - u_l)^2}{\sigma} = \frac{\rho_g}{\rho_l} We_l = 38 \tag{33}$$

So this result is consistent with the range as shown in Table 2. When M is tending toward zero, the bag-type breakup should disappear, and the membrane-fiber breakup should still appear.

The upstream geometries for air and water flow passages have effect on turbulence intensity (root mean square velocity) and boundary layer thickness. There is the corresponding introduction in the literature.[31] For instance, the turbulence intensity of long coaxial cylinders is bigger than the coaxial convergent injectors. So the convergent nozzle is common in scientific and engineering applications. The influence of turbulence intensity on atomization is very useful and has been investigated in the literature.[2,17,32,33] However, this detailed physical mechanism has not been completely known. We also hope to investigate the influence on liquid breakup morphology and mechanism in the future.

Figure 13. Membrane-fiber breakup of high-speed round liquid jet in still gas. ($We = 38$)[30]

Conclusions

In this article, the properties of seven coaxial twin-fluid air-blast atomizers with water–air systems have been investigated. The following conclusions are deduced here:

The membrane-type breakup can be divided into two subregimes called bag-type breakup and membrane-fiber breakup according to their different breakup morphology. The correlation of characteristic length in bag-type breakup is obtained, which decreases with the atomizer exit area ratio A_l/A_g and M. Influence of GLR and A_l/A_g on the breakup morphology of liquid jet is studied. To obtain reasonable atomization morphology criterions, we suggest using the atomizer exit area ratio to modify Weber number and momentum flux ratio per unit volume. In the new map of the parameter space We_m–M_m, all important parameters on nozzle size are considered. This We_m–M_m map is also consistent with the experimental results in the literature. At last, the results show the transition Weber number of breakup regimes of coaxial water–air jets is very close to the liquid jet in cross air flow and secondary atomization, which strongly supports the self-similar phenomenon of atomization.

Acknowledgments

This study was supported by the National Natural Science Foundation of China (21176079), National Development Programming of Key Fundamental Researches of China (2010CB227005), Fundamental Research Funds for the Central Universities (WB1314046), and National Science Foundation for Post-doctoral Scientists of China (2012M520848).

Notation

A_l = area of water exit (central circular orifice) of atomizer
A_g = area of gas exit (annular orifice) of atomizer
D = diameter of atomizer central water circular orifice
D_i = inner diameter of atomizer coaxial air annular orifice
D_o = outer diameter of atomizer coaxial air annular orifice
E_t = total input energy supplied by airflow
E_0 = the energy supplied by airflow which is used to accelerate the liquid
E_1 = the energy supplied by airflow which is needed by water jet breakup
E_2 = the energy supplied by airflow when A_l/A_g is small
E_3 = the energy of dissipation of the surrounding still air
GLR = gas to liquid mass ratio
K = a correction factor
k = a correction factor
L = liquid jet characteristic length

M = momentum flux mass ratio per unit volume (or called momentum flux ratio)
M_c = critical M of bag-type breakup appearing
M_m = modified M using A_l/A_g
Re = liquid Reynolds number
Re_g = gas Reynolds number
SMD = Sauter mean diameter
u_g = gas velocity
u_l = liquid velocity
We = gas Weber number
We_l = liquid Weber number
We_m = modified We using A_l/A_g
We_t = transition Weber number between different breakup modes
We_0 = the transition We when A_l/A_g is small or GLR is big
We_1 = transition Weber number between Rayleigh breakup and bag breakup in view of GLR
We_2 = transition Weber number between bag breakup and membrane-fiber regime at $M > 0.08$ in view of GLR
We_3 = transition Weber number between membrane-fiber regime and fiber breakup at $M > 0.08$ in view of GLR
We_4 = transition Weber number between Rayleigh breakup and membrane-fiber regime at $M < 0.08$ in view of GLR
We_5 = transition Weber number between membrane-fiber regime and fiber breakup at $M < 0.08$ in view of GLR
We_6 = transition Weber number between Rayleigh breakup and bag breakup in view of A_l/A_g
We_7 = transition Weber number between bag breakup and membrane-fiber regime at $M > 0.08$, transition Weber number between Rayleigh breakup and membrane-fiber regime at $M < 0.08$ in view of A_l/A_g
We_8 = transition Weber number between membrane-fiber regime and fiber breakup in view of A_l/A_g
x = a correction factor
ρ_l = liquid density
ρ_g = gas density
σ = surface tension
μ_l = liquid dynamic viscosity
μ_g = gas dynamic viscosity

Literature Cited

1. Rayleigh L. On the instability of jets. *Proc London Math Soc*. 1878; 10:4–13.
2. Hinze JO. Fundamentals of the hydrodynamic mechanism of splitting in dispersion processes. *AIChE J*. 1955;1:289–295.
3. Reitz RD, Bracco FV. Mechanism of atomization of a liquid jet. *Phys Fluids*. 1982;25:1730–1742.
4. Lefebvre AH. *Atomization and Sprays*. New York: Hemisphere, 1989.
5. Villermaux E. Unifying ideas on mixing and atomization. *New J Phys*. 2004;6:125.
6. Liu HF, Gong X, Li WF, Wang FC, Yu ZH. Prediction of droplet size distribution in sprays of prefilming air-blast atomizers. *Chem Eng Sci*. 2006;61:1741–1747.
7. Lasheras JC, Hopfinger EJ. Liquid jet instability and atomization in a coaxial gas stream. *Annu Rev Fluid Mech*. 2000;32:275–308.
8. Villermaux E. Fragmentation. *Annu Rev Fluid Mech*. 2007;39:419–446.
9. Gorokhovski M, Herrmann M. Modeling primary atomization. *Annu Rev Fluid Mech*. 2008;40:343–366.
10. Dumouchel C. On the experimental investigation on primary atomization of liquid streams. *Exp Fluids*. 2008;45:371–422.
11. Portoghese F, House P, Berruti F, Briens C, Adamiak K, Chan E. Electric conductance method to study the contact of injected liquid with fluidized particles. *AIChE J*. 2008;54:1770–1781.
12. Sarchami A, Ashgriz N, Tran H. An atomization model for splash plate nozzles. *AIChE J*. 2010;56:849–857.
13. Lim LK, Hua JS, Wang CH, Smith KA. Numerical simulation of cone-jet formation in electrohydrodynamic atomization. *AIChE J*. 2011;57:57–78.
14. Addo-Yobo FO, Pitt MJ, Obiri HA. The effects of particle size on the mechanisms of atomization of suspensions using hydraulic spray nozzles. *AIChE J*. 2011;57:2007–2024.
15. Rodriguez-Rivero C, Del Valle EMM, Galan MA. Development of a new technique to generate microcapsules from the breakup of non-Newtonian highly viscous fluid jets. *AIChE J*. 2011;57:3436–3447.
16. Farago Z, Chigier N. Morphological classification of disintegration of round liquid jets in a coaxial air stream. *Atom Sprays*. 1992;2: 137–153.
17. Lasheras JC, Villermaux E, Hopfinger EJ. Break-up and atomization of a round water jet by a high-speed annular air jet. *J Fluid Mech*. 1998;357:351–379.
18. Leroux B, Delabroy O, Lacas F. Experimental study of coaxial atomizers scaling. *Part I: Dense core zone*. *Atom Sprays*. 2007;17: 381–407.
19. Wang YJ, Kyoung SI, Kamel F. Similarity between the primary and secondary air-assisted liquid jet breakup mechanism. *Phys Rev Lett*. 2008;100:154502.
20. Baillot F, Blaisot JB, Boisdron G, Dumouchel C. Behaviour of an air-assisted jet submitted to a transverse high-frequency acoustic field. *J Fluid Mech*. 2009;640:305–342.
21. Shi XD, Brenner MP, Nagel SR. A cascade of structure in a drop falling from a faucet. *Science*. 1994;265:219–222.
22. Eggers J. Nonlinear dynamics and breakup of free-surface flows. *Rev Mod Phys*. 1997;69:865–930.
23. Liu HF, Li WF, Gong X, Cao XK, Xu JL, Chen XL, Wang YF, Yu GS, Wang FC, Yu ZH. Effect of liquid jet diameter on performance of coaxial two-fluid air-blast atomizers. *Chem Eng Prog*. 2006;45: 240–245.
24. Jiang DJ, Liu HF, Li WF, Xu JL, Wang FC, Gong X. Modeling atomization of a round water jet by a high-speed annular air jet based on the self-similarity of droplet breakup. *Chem Eng Res Des*. 2012;90:185–192.
25. Kline SJ, McClintock FA. Describing uncertainties in single-sample experiments. *Mech Eng*. 1953;75(1):3–8.
26. Cohen RD. Effect of viscosity on drop breakup. *Int J Multiphase Flow*. 1994;20:211–216.
27. Rizk NK, Lefebvre AH. Spray characteristics of plain-jet airblast atomizers. *J Eng Gas Turbines Power*. 1984;106(3):634–638.
28. Sallam KA, Aalburg C, Faeth GM. Breakup of round nonturbulent liquid jets in gaseous cross flows. *AIAA J*. 2004;42:2529–2540.
29. Guildenbecher DR, López-Rivera C, Sojka PE. Secondary atomization. *Exp Fluids*. 2009;6:371–402.
30. Sallam KA, Dai Z, Faeth GM. Liquid breakup at the surface of turbulent round liquid jets in still gases. *Int J Multiphase Flow*. 2002; 28:427–449.
31. Marmottant P, Villermaux E. On spray formation. *J Fluid Mech*. 2004;498:73–111.
32. Mayer WOH. Coaxial atomization of a round liquid jet in a high speed gas stream: A phenomenological study. *Exp Fluids*. 1994; 16(6):401–410.
33. Rehab H, Villermaux E, Hopfinger EJ. Flow regimes of large-velocity-ratio coaxial jets. *J Fluid Mech*. 1997;345(1):357–381.

Manuscript received Aug. 2, 2012, and revision received Dec. 29, 2013.